Proceedings of the 17th World Congress
The International Federation of Automatic Control
Seoul, Korea, July 6-11, 2008

On Modeling and Parameter Estimation of Brushless DC Servoactuators for Position Control Tasks ⋆

Ricardo Campa, Elio Torres, Francisco Salas, and Víctor Santibáñez

Instituto Tecnológico de la Laguna, Blvd. Revolución y Cuauhtémoc, Torreón, Coah., 27000, Mexico (e-mail: recampa@itlalaguna.edu.mx)

Abstract: Brushless DC (BLDC) servomotors have become a popular choice when implementing high–precision position controllers for mechatronic systems. A motor of this kind requires a drive that can be configured in different operation modes, according to the internal controllers it utilizes. This paper first describes the main features and the complete electromechanical model of a BLDC motor/drive system, including some procedures for the identification of its parameters. Three common schemes for implementing position control using this kind of actuators are also presented, and the equivalence among them is employed to determine the drive's internal control gains. Finally, experimental results in a typical BLDC servoactuator allow us to show the significance of the estimated parameters in real position control tasks.

1. INTRODUCTION

The so–called *brushless DC* (*BLDC*) motors are broadly used as actuators in electromechanical systems requiring high–precision motion control tasks. Typical applications include robotic arms (Kawasaki [2001], Mitsubishi [2002]), conveyors, and positioning systems (Oriental [2007]). They are also used in research laboratories worldwide (e.g. Reyes and Kelly [1997], Dawson et al. [1998]).

A BLDC servoactuator is composed by a 3–phase permanent magnet synchronous machine and an electronic drive, which produces the required 3–phase power signals. The name BLDC comes from the fact that its steady–state response is similar to the one of a brushed DC motor (Krause et al. [2002]).

The drive of a BLDC motor can include up to four sections, as shown in Figure 1: a voltage inverter, a torque controller, a velocity controller and a position controller (Krause et al. [2002], Parker [1998]). The three latter constitute a hierarchical control scheme, with nested control loops. In most of the cases it is possible to configure the drive so that its input signal corresponds to either the motor's desired position, velocity or torque (q_d, ω_d or τ_d, respectively, in Figure 1). Thus, there exist three *operation modes*, indicated by dashed lines in the same figure.

When using BLDC motors, the position control aim can be achieved in various forms. The simplest is to configure the drive directly in *position mode*; the drawback of this scheme is that, in general, it is not possible to change the internal position controller or its gains. Other way is to configure the drive in *velocity mode* and implement an external position controller that generates the desired velocity references for the drive. Finally, the drive can be configured in *torque mode*, requiring the design of an external position controller to generate the desired torque.

A special kind of BLDC servomotors are those used for "direct–drive" applications, that is, where the rotors of the motors are directly coupled to the load, without using gear trains or any other kind of transmission. As high torque is required in these so–called *brushless direct–drive* (BLDD) motors, most of them are of outer–rotor type. Well–known examples of these are Parker's Dynaserv (Parker [1998]), and NSK's Megatorque series (Bona et al. [2003]).

The aim of this paper is threefold. First, we recall the electromechanical model of the BLDC motor and its drive. Second, we show some typical position control schemes that can be implemented with it. Third, we give some guidelines for the estimation of both the motor parameters and the drive's internal control gains. At the end, we include some experimental results showing the application of these techniques in a real BLDC motor.

2. MODELING OF BLDC SERVOACTUATORS

2.1 Motor model

The model of a BLDC motor can be divided into its mechanical and electrical parts (Campa et al. [2005]). Let $q, \dot{q}, \ddot{q}$ be, respectively, the angular position, velocity and acceleration of the motor shaft, then

$$J\ddot{q} + f(\dot{q}) + l(q) = \tau, \tag{1}$$

where J is the rotor inertia, τ is the mechanical torque applied to the motor, and $f(\dot{q})$, $l(q)$, are functions representing the friction and load torques, respectively. For the purpose of this paper we consider the simplest, viscous friction model, given by

$$f(\dot{q}) = f_v\dot{q},$$

where f_v is the viscous friction parameter. The load torque function $l(q)$ is specially important when the BLDC

⋆ This work was partially supported by DGEST and CONACyT–Mexico (grant No. 60230).

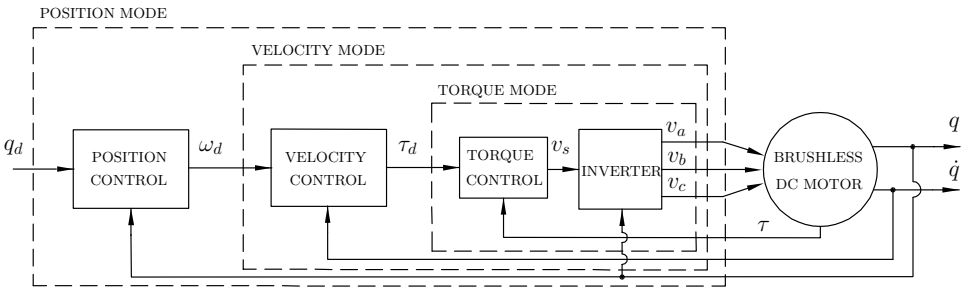

Fig. 1. General block diagram of a BLDC servoactuator system

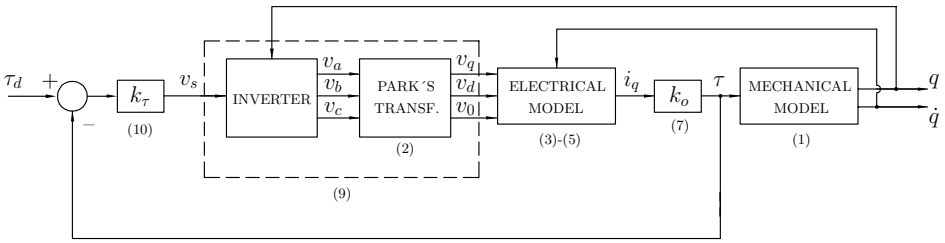

Fig. 2. Simplified transformed model of the BLDC motor/drive in torque mode.

motor is used in robotic applications; for example, in a pendulum–like vertical load, it has the form $l(q) = M\sin(q)$, where M is a positive constant.

Regarding the electrical model, we consider the one in (Dawson et al. [1998]), which uses the so–called Park's transformation (Krause et al. [2002]), given by:

$$\begin{bmatrix} v_q \\ v_d \\ v_o \end{bmatrix} = \sqrt{\frac{2}{3}} \begin{bmatrix} \cos(\phi) & \cos\left(\phi - \frac{2\pi}{3}\right) & \cos\left(\phi + \frac{2\pi}{3}\right) \\ \sin(\phi) & \sin\left(\phi - \frac{2\pi}{3}\right) & \sin\left(\phi + \frac{2\pi}{3}\right) \\ \frac{1}{\sqrt{2}} & \frac{1}{\sqrt{2}} & \frac{1}{\sqrt{2}} \end{bmatrix} \begin{bmatrix} v_a \\ v_b \\ v_c \end{bmatrix} \quad (2)$$

to simplify the model, converting the motor's input phase voltages $\{v_a, v_b, v_c\}$, into the transformed voltages $\{v_q, v_d, v_o\}$. Angle ϕ represents the rotor electrical displacement, given by $\phi = n_p q$, where n_p is the number of permanent magnet pole pairs in the motor.

The transformed electrical model of the motor becomes:

$$L_q \frac{d\, i_q}{dt} + R_s i_q = v_q - n_p \left(L_d\, i_d + \lambda_m\right) \dot{q}, \quad (3)$$

$$L_d \frac{d\, i_d}{dt} + R_s i_d = v_d + n_p L_q i_q \dot{q}, \quad (4)$$

$$L_o \frac{d\, i_o}{dt} + R_s i_o = v_o \quad (5)$$

where $\{i_q, i_d, i_o\}$ are the transformed currents, obtained from $\{i_a, i_b, i_c\}$ using a transformation similar to (2); R_s is the phase resistance; λ_m is a constant representing the magnetic flux linkage due to the permanent magnet; L_q, L_d, L_o are the so–called *synchronous inductances*, which are obtained by transforming the self and mutual inductances of the rotor coils.

It can be shown that if the 3–phase system is balanced, then $v_o = 0$, $i_o = 0$, and the electrical model reduces to equations (3) and (4). Furthermore, the relation between the electrical model and the mechanical model (1) is established through the electrical torque, which must be equal to the mechanical torque, and is given by

$$\tau = n_p \left(\lambda_m\, i_q + \left[L_d - L_q\right] i_q\, i_d\right). \quad (6)$$

As pointed out by Krause et al. [2002], most of BLDC motors have synchronous inductances with very similar values. Considering $L_q = L_d$, then, from (6):

$$\tau = k_o i_q \quad (7)$$

where

$$k_o = n_p \lambda_m. \quad (8)$$

2.2 Drive model

Even though the drive model depends on the type of inverter employed, it is possible to assume that the inverter is an ideal voltage source (Krause et al. [2002]), leading to consider that, by applying Park's transformation, the inputs of the motor are v_q, v_d and v_o, satisfying:

$$\begin{bmatrix} v_q \\ v_d \\ v_o \end{bmatrix} = \begin{bmatrix} k_s \\ 0 \\ 0 \end{bmatrix} v_s \quad (9)$$

where k_s is a factor depending on the inverter type, and v_s is its voltage input.

As explained in (Parker [1998]) the torque controller is typically a proportional (P) controller, so that we can write:

$$v_s = k_\tau \left(\tau_d - \tau\right) \quad (10)$$

where k_τ is the torque proportional gain and τ corresponds to (7). Figure 2 shows the simplified model given by equations (1)-(5), (7), and (9)-(10). The number under each block in the figure indicates the corresponding equation.

The drive's inner velocity controller usually can be chosen as one of the following:

- P velocity controller:

$$\tau_d = k_{vo} \widetilde{\omega} \quad (11)$$

- PI velocity controller:

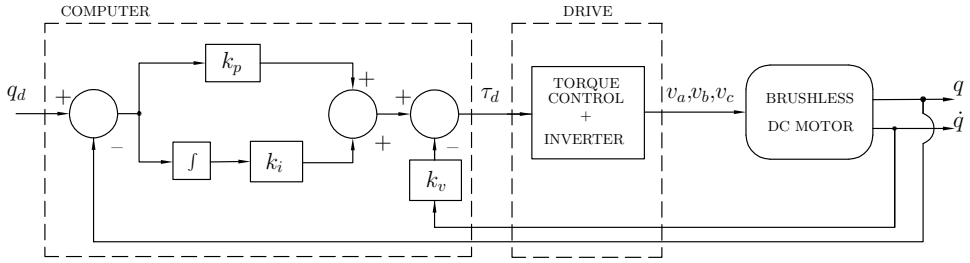

Fig. 3. Position PID controller (torque mode).

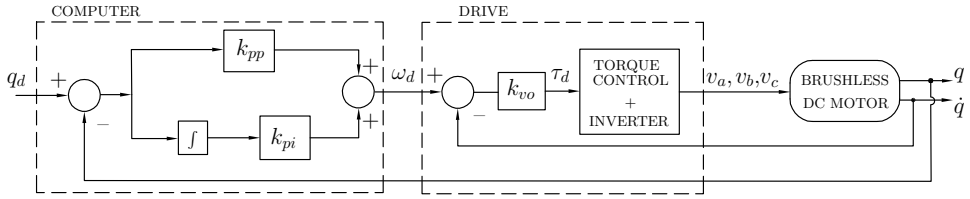

Fig. 4. Position PI + velocity P controller (velocity mode).

$$\tau_d = k_{vp}\widetilde{\omega} + k_{vi}\xi \tag{12}$$

$$\xi = \int_0^t \widetilde{\omega}(t)dt \tag{13}$$

where

$$\widetilde{\omega} = \omega_d - \dot{q} \tag{14}$$

is the velocity error. For the purpose of this paper, the drive's inner position controller is not considered.

3. POSITION CONTROL SCHEMES

In this section we describe three position control schemes that can be employed in a BLDC servoactuator. These are:

- Position PID control.
- Position PI + velocity P (PI-P) control.
- Position P + velocity PI (P-PI) control.

The traditional position PID control is intended to deliver a desired torque to the inner torque control loop of the drive (configured in torque mode). The latter two controllers use a two–loop control scheme where the outer position controller produces the desired velocity for the inner velocity controller. Even though these controllers can be implemented completely by the user, in order to apply the gain estimation procedure described in Section 5 we chose to configure the drive in velocity mode.

3.1 PID control

Figure 3 shows the block diagram of a traditional PID control, such as the one analyzed in (Kelly and Moreno [2001]), consisting of a PI position loop, plus a velocity feedback.

The control law is

$$\tau_d = k_p\tilde{q} + k_i\eta - k_v\dot{q} \tag{15}$$

$$\eta = \int_0^t \tilde{q}(t)dt \tag{16}$$

where $\tilde{q}$ is the position error, defined by

$$\tilde{q} = q_d - q. \tag{17}$$

Also note that, if q_d is constant, then the derivative of (17) becomes

$$\dot{\tilde{q}} = -\dot{q}. \tag{18}$$

and the last term in (15) can be rewritten as $+k_v\dot{\tilde{q}}$.

3.2 PI-P control

As shown in Figure 4, this controller consists of two control loops: an outer position proportional–integral (PI) loop and an inner velocity proportional (P) loop.

The velocity controller is given by equations (11) and (14). The position controller is

$$\omega_d = k_{pp}\widetilde{q} + k_{pi}\eta \tag{19}$$

where η is defined in (16).

Substituting (19) in (14), and then in (11), we get

$$\tau_d = k_{vo}\left(k_{pp}\tilde{q} + k_{pi}\eta - \dot{q}\right)$$

which has the same form as (15), but now with

$$k_p = k_{pp}k_{vo}, \tag{20}$$

$$k_i = k_{pi}k_{vo}, \tag{21}$$

$$k_v = k_{vo}. \tag{22}$$

3.3 P-PI control

Figure 5 shows the block diagram for this controller. It is a proportional position controller, plus an inner PI velocity loop, and it is similar to the one studied by (Kelly and Moreno [2001]), for the regulation case.

The control law for this controller is obtained from equations (12)-(14), relating to the inner velocity loop and

$$\omega_d = k_{po}\tilde{q} \tag{23}$$

for the outer position loop, where the position error $\tilde{q}$ was previously defined in (17).

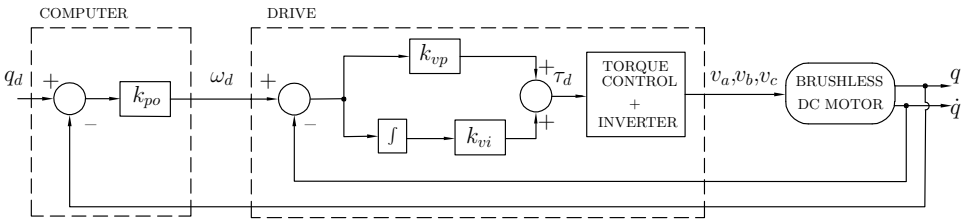

Fig. 5. Position P + velocity PI controller (velocity mode).

Now, combining (14) and (23), we have

$$\widetilde{\omega} = k_{po}\tilde{q} - \dot{q} \tag{24}$$

and (13) becomes

$$\xi = \int_0^t (k_{po}\tilde{q}(t) - \dot{q}(t))\, dt,$$

which can be rewritten as

$$\xi = k_{po}\eta + \tilde{q} \tag{25}$$

using (16) and (18).

Finally, substituting (24) and (25) in (12), the P-PI control law can be written as

$$\tau_d = k_p\tilde{q} + k_i\eta - k_v\dot{q}$$

where now

$$k_p = k_{po}k_{vp} + k_{vi}, \tag{26}$$

$$k_i = k_{po}k_{vi}, \tag{27}$$

$$k_v = k_{vp}. \tag{28}$$

A conclusion is that the three control schemes studied in this section have the same PID structure, and thus they are equivalent.

4. MOTOR PARAMETER IDENTIFICATION

To completely characterize a BLDC motor, we need to identify all the parameters in its electromechanical model. Specifically, we should estimate both the mechanical parameters $\{J, f_v\}$, and the electrical parameters $\{R_s, n_p, \lambda_m, L_q, L_d\}$.

The rotor inertia J is usually given by the motor's manufacturer. In the following, some simple procedures for obtaining the rest of the parameters are given. A more detailed description of these methods can be found in (Campa et al. [2005]).

4.1 Viscous friction (f_v)

We refer to the simple procedure for obtaining both viscous and Coulomb friction parameters that was proposed by Kelly et al. [2000].

4.2 Phase resistance (R_s)

This parameter can be easily obtained from direct measurements using an ohmmeter; we only need to know the type of connection ("Y" or "Δ") of the 3–phase motor windings. Assuming that the three phases are balanced (i.e., they have the same impedance) the following simple procedure allows to determine both, the type of connection and R_s:

a) Measure the resistance between two motor lines: R_1
b) Join two lines together and measure the resistance between this joint and the other (untied) line: R_2
c) Obtain the ratio $c = \frac{R_2}{R_1}$.

If the motor has a Y–connection then $c = 0.75$ and $R_s = \frac{R_1}{2}$; if it is Δ–connected then $c = 0.5$ and $R_s = R_1$.

4.3 Number of pole pairs (n_p) and PM flux linkage (λ_m)

Both the number of pole pairs of the rotor and the permanent–magnet flux linkage can be obtained from the same experiment, operating the motor in generator mode, that is, using a mechanical coupling (usually a DC brushed motor) to externally rotate the BLDC motor with open terminals (lines). The induced voltage between two lines should be seen employing an oscilloscope.

Let ν_m and ν_e be, respectively, the mechanical frequency (speed) of the rotor, in revolutions per second, and the electrical frequency of the corresponding induced voltage, in cycles per second. Then, by rotating the BLDC motor at a given speed ν_m, it is possible to measure ν_e from the sinusoidal signal in the oscilloscope. The number of pair poles si simply

$$n_p = \frac{\nu_e}{\nu_r}. \tag{29}$$

The PM flux linkage, λ_m can be obtained from the following formula (Ohm [2000]), which employs the measured peak value of the voltage induced between two lines, V_p, when the rotor is moving at a constant speed:

$$\lambda_m = \frac{V_p}{2\sqrt{3}\pi\nu_e}. \tag{30}$$

4.4 Synchronous inductances (L_d, L_q)

The so–called synchronous inductances L_d and L_q, correspond to the equivalent inductances of the stator phase windings when the rotor is aligned to the transformed *direct* (d) and *quadrature* (q) axes, respectively (Krause et al. [2002]). Due to the permanent magnet distribution and the rotor structure (with saliencies) these inductances are in general different. However, in this paper we consider the case where $L_d = L_q$.

There are several methods to obtain the synchronous inductances indirectly from step or frequency responses. For our purposes, notwithstanding, we rely on the use of a commercial inductance meter. Two of the motor 3–phase

lines are tied together and the inductance meter is used to measure the inductance between the joint and the other (untied) line. If this inductance is named L_m, then we have, for the simplified case:

$$L_d = L_q = \frac{2}{3} L_m$$

A more general procedure for obtaining L_d and L_q is explained in (Campa et al. [2005]).

5. DRIVE GAIN ESTIMATION

Regarding the drive model, we are interested in estimating the inverter gain k_s, the torque control gain k_τ, and the velocity control gains k_{vo}, k_{vp} and k_{vi}.

As mentioned in Section 2.2, the inverter gain k_s strongly depends on the type of voltage inverter the drive uses. Some approximations of this parameter for ideal inverters can be found in (Krause et al. [2002]).

5.1 Torque proportional control gain (k_τ)

For estimating this gain we refer to the procedure proposed in (Campa et al. [2005]), which considers the ideal case of steady–state operation (i.e., constant speed motion) when a constant torque input τ_d is applied to the motor, configured in torque mode. Now, for a given τ_d, three measurements should be done:

- The steady–state rotor speed: ν_{ss}.
- The rms value of the phase current: I_s.
- The rms value of the line–to–line voltage: V_{ll}.

The value of drive gain k_τ can now be estimated, by solving from (10):

$$k_\tau = \frac{v_s}{\tau_d - k_o i_q} \tag{31}$$

where (7) was employed. Gain k_o was defined in (8); the values of v_s and i_q in steady–state can be obtained from the measurements taken, as follows (Campa et al. [2005]):

$$i_q = \frac{\sqrt{2} I_s R_s^2}{R_s^2 + n_p^2 L^2 \nu_{ss}^2}, \qquad v_s = \frac{\sqrt{2}}{\sqrt{3}} V_{ll}.$$

where $L = L_d = L_q$.

5.2 Velocity control gains (k_{vo}, k_{vp}, k_{vi})

We now propose a practical method to estimate the drive inner velocity control gains. This method starts from the fact that, even though the three control schemes introduced in Section 3 are implemented differently, they have the same PID structure. So, by a proper selection of the outer position control gains, it should be possible to get similar responses of the rotor position, using the three cases. Equal responses (in the ideal case) mean that the PID control gains are equivalent, i.e. that equations (20)-(22) and (26)-(28) are satisfied.

The procedure for estimating the inner control gains, and tuning the outer ones, in order to obtain similar responses is explained below.

1. Configure the drive in velocity mode and implement the P-PI control scheme. Now, select a gain k_{po} that allows to get an acceptable rotor position response.
2. Configure the drive in torque mode and implement the PID scheme. In this case, considering that equations (26)-(28) should be satisfied, the P, I and D gains can be adjusted in terms of k_{vi} and k_{vp}, which can be seen as free parameters (k_{po} is already known). One should choose k_{vi} and k_{vp} so as to get a motor response as similar as possible to the one in step 1.
3. Note that, as a result from the previous step, not only an estimation of the inner velocity PI controller is done, but we also obtained the values of the PID control gains (k_p, k_v, k_i), by means of (26)-(28).
4. Finally, taking the computed values of k_p, k_v and k_i, it is possible to solve (20)-(22) to determine k_{vo}, k_{pp} and k_{pi}.

6. EXPERIMENTAL EVALUATION

The identification methods proposed in the previous sections were employed to characterize a BLDC motor we have in our laboratory. The motor is a Dynaserv DM1004C from Parker/Compumotor, with maximum torque of 4 Nm and maximum velocity of 150 rpm (15.7 rad/s). The rotor is outer–type, with nominal inertia $J = 0.0025$ kg·m^2. The matching drive (model SM1004C) can be configured in either torque, velocity or position modes.

Angular position measurements of the rotor are possible thanks to a high–resolution optical encoder (655,360 pulses per revolution) in the shaft, and a PC acquisition board with encoder inputs (PCI–MultiQ, from Quanser). Rotor velocity is computed in the PC via numerical derivation of the position using a simple Euler algorithm. The acquisition board I/O signals are processed at a sampling period of 1 ms by using WinMechLab, a real–time control system running under Windows XP (Campa et al. [2004]).

Table 1 summarizes the values of the parameters for the DM1004C motor, which were obtained using the procedures in Section 4.

Table 1. Identified parameters for DM1004C

Parameter	Symbol	Value	Units
Rotor inertia	J	0.0025	kg·m^2
Viscous friction	f_v	0.203	N·m·s
Phase resistance	R_s	1.9	Ω
No. of pole pairs	n_p	120	
PM flux linkage	λ_m	0.0106	Wb
Synch. inductances	L_d, L_q	0.00654	H

Regarding the computation of the drive's inner velocity control gains, we use the procedure in Section 5.2. To this end, the same regulation control task was considered for the three schemes: to take the rotor from its initial position at rest ($q = 0$), in $t = 0$, to a desired position $q_d = 60°$ (1.05 rad), without overshooting. Figure 6 shows the position errors ($\tilde{q} = q_d - q$) obtained using the three analyzed schemes after tuning the gains. It is interesting to observe the great similarity among the responses even though the controllers are implemented differently. The estimated drive gains are given in Table 2.

In order to evaluate the accuracy in the characterization of the DM1004C motor, we completed some simulations, using the identified parameters. The simulation results were then compared with similar experiments carried out on the

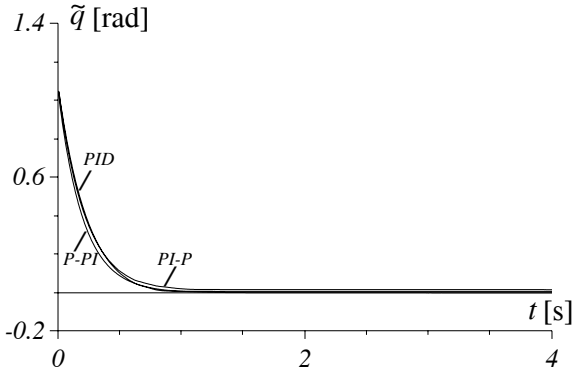

Fig. 6. Position errors for the three PID–like controllers.

Table 2. Identified parameters for the drive

Parameter	Symbol	Value	Units
Inverter gain	k_s	1	
Torque gain	k_τ	549	V/Nm
Vel. proportional gain	k_{vo}	1.9	Nms/rad
Vel. PI proportional gain	k_{vp}	1.9	Nms/rad
Vel. PI integral gain	k_{vi}	0.95	Nm/rad

actual motor/drive system. As an example, Figure 7 shows the comparison of simulated and experimental velocity responses for a square–wave torque input in the drive (configured in torque mode). The experimental result is labeled "E". Two type of simulations are considered: simulation labeled "EMS" is made employing the complete (electrical and mechanical) model, while simulation labeled "MS" uses only the mechanical model (i.e., considering that $\tau = \tau_d$, in Figure 2).

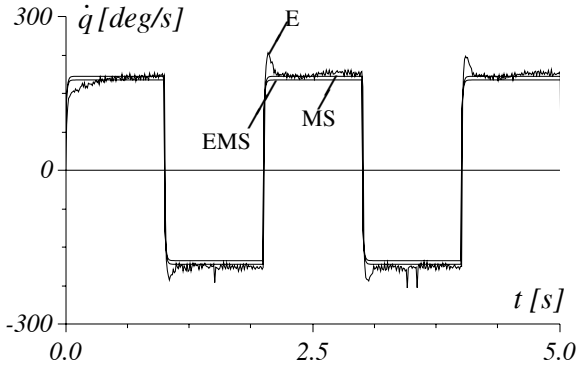

Fig. 7. Motor's velocity response to a square–wave torque input (E: experimental, MS and EMS: simulated).

It can be noted in Figure 7 that simulation results are very alike to each other, and to the experiment. This implies that the inner torque controller makes the motor output torque τ track the desired torque τ_d. Note that, in the case of exact tracking, the electrical model can be discarded. This result confirms the common idea of considering only the mechanical model, when analyzing BLDC motors.

7. CONCLUSION

Nowadays, brushless direct–drive (BLDC) servomotors are of interest since they are commonly used in several applications of high–precision position control. By using Park's transformation for synchronous machines, the mathematical model of a BLDC motor/drive system becomes similar to the one of a brushed DC motor.

This paper has recalled both the derivation of the complete electromechanical model of a BLDC servomotor, and some techniques for the estimation of its parameters. In addition, we studied three common position control schemes that can be implemented with BLDC motors; after showing that these controllers are equivalent, we used this fact to develop an experimental procedure to estimate the drive's internal velocity control gains.

To show the validity of our approach, we used the proposed procedures for the identification of the motor/drive parameters in a real servoactuator. At the end, simulations were carried out and compared with experimental results, showing a good performance.

REFERENCES

B. Bona, M. Indri, and N. Smaldone. Nonlinear friction estimation for digital control of direct–drive manipulators. *Proc. of the 2003 European Control Conference*, Cambridge, UK, September 2003.

R. Campa, R. Kelly, and V. Santibañez. Windows–based real–time control of direct–drive mechanisms: platform description and experiments. *Mechatronics*, Vol. 14, No. 9, pp. 1021-1036, 2004.

R. Campa, E. Torres, V. Santibáñez and R. Vargas. Electromechanical dynamics characterization of a brushless direct-drive servomotor. *Proc. of the VII Mexican Congress on Robotics (COMRob2005)*, Mexico, D. F., October 2005.

D. Dawson, J. Hu and T.C. Burg. *Nonlinear Control of Electric Machinery*. Marcel Dekker, 1998.

Kawasaki Robotics. C Series Controller Electrical Maintenance Manual MPECCON118E-4. Kawasaki Robotics USA, 2001.

R. Kelly, J. Llamas and R. Campa. A measurement procedure for viscous and Coulomb friction. *IEEE Transactions on Instrumentation and Measurement*, Vol. 49, No. 4, pp. 857-861, 2000.

R. Kelly, and J. Moreno. Learning PID structures in an introductory course of automatic control. *IEEE Transactions on Education*, Vol. 44, pp. 373-376, 2001.

P.C. Krause, O. Wasynczuk, and S. D. Sudhoff. *Analysis of Electric Machinery and Drive Systems*. Wiley-Interscience, 2002.

Mitsubishi Heavy Industries, Ltd. Instruction Manual for Servo Driver. General Purpose Robot PA10 Series, 2002.

Oriental Motor. AC & Brushless DC Speed Control Motor Systems In *http://www.orientalmotor.com/products /ac-dc-speed-motors/index.htm*, 2007.

Parker Automation. Compumotor's Virtual Classroom. CD-ROM, Compumotor's catalog, 1998.

F. Reyes, and R. Kelly. Experimental evaluation of identification schemes on a direct drive robot. *Robotica*, Vol. 15, pp. 563-571, 1997.

D.Y. Ohm, Dynamic model of PM synchronous motors. Drivetech Inc., Technical Article, 2000 (in `http://www.drivetechinc.com/ id16.html`).